

Study on the fabrication and investigation of the structural, optical and photocatalytic properties of Co^{2+} , Ni^{2+} co-doped ZnO nanomaterials

Ta Ngoc Dung, Nguyen Thi Tuyet Mai*, Huynh Dang Chinh

ABSTRACT

In this study, Co^{2+} , Ni^{2+} co-doped ZnO nanomaterials (Co,Ni-ZnO NMs) were successfully fabricated by hydrothermal method at low temperature at 90°C for 12 hours. Co^{2+} and Ni^{2+} ions were doped into the ZnO nanomaterials at ratios of 1 mol% and 2 mol%, respectively (calculated compared to the number of moles of Zn^{2+}). The methods used to study on the structure and properties of materials such as XRD, SEM/EDX and UV-vis spectra. The results showed that the fabricated materials were in the form of wurtzite single-phase and nanometer structure. The optical band gap energy (E_g) of Co, Ni-ZnO NMs was determined based on the Kubelka–Munk equation and achieved a the value of 3.17 eV. The E_g of undoped ZnO was about of 3.34 eV. Reducing this optical gap energy of the material is desirable in research on semiconductor materials with the aim to improve the applicability of materials that are responsive under irradiation of light shifted to visible region. Besides, the results also showed that the ZnO nanomaterials co-doped with Co^{2+} and Ni^{2+} achieved a photocatalytic efficiency for degradation of the methylene blue (MB) dye solution in the visible light regions. Thus, ZnO material co-doped with Co^{2+} and Ni^{2+} ions has achieved superiority in optical applications stimulated by visible light (undoped ZnO material only achieves optical applications in the ultraviolet light region). The rate constant for the MB dye photocatalytic decomposition reaction had been determined according to the Langmuir Hinshelwood (L-H) kinetic model. This decomposition rate constant of the fabricated samples all complied with the first-order kinetic model with a high R^2 correlation coefficient (achieved above of 0.92). The rate constant of the Co,Ni-ZnO NMs sample was approximately 17.8 times larger than that of the undoped ZnO sample (achieved 0.006204 and 0.0003471 min^{-1} , respectively).

Key words: Wurtzite ZnO nanostructure, Co^{2+} , Ni^{2+} co-doped ZnO, Kubelka–Munk, visible light irradiation

School of Chemistry and Life Science,
Hanoi University of Science and
Technology, No. 1 Dai Co Viet, Hanoi,
Vietnam

Correspondence

Nguyen Thi Tuyet Mai, School of
Chemistry and Life Science, Hanoi
University of Science and Technology,
No. 1 Dai Co Viet, Hanoi, Vietnam

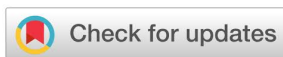
Email: mai.nguyenthituyet@hust.edu.vn

History

- Received: 01-10-2023
- Accepted: 10-1-2024
- Published Online: 31-3-2024

DOI :

<https://doi.org/10.32508/stdjet.v6iS13.1256>



Copyright

© VNUHCM Press. This is an open-access article distributed under the terms of the Creative Commons Attribution 4.0 International license.



INTRODUCTION

The environmental pollution, especially water pollution, is a global issue. Organic dyes are one of the pollutants that have durability and high temperature stability, colorant, potentially carcinogenic and toxic. These pollutants release into the environment lead to health, aesthetical and serious environmental threats. Therefore, their removal from the industrial wastewater sources is a very necessary¹⁻⁷. Currently, in applied research to treat organic dyes in wastewater, attention is often paid to using two main types of materials: adsorbent and photocatalytic materials⁸⁻¹². In addition, the ZnO semiconductor is also a good photocatalytic material for environmental treatment. ZnO nanostructured material is characterized as a group II-IV semiconductor with a wide optical gap (3.37 eV) and large excitation binding energy (60 meV)¹³⁻¹⁷. ZnO nanomaterials also have the advantages of having many di-

verse shapes such as nanorods, nanowires, nanofibers, nanospheres, nanosheets, nanoscales, nanotubes, flower shape,...¹⁸⁻²². Materials fabricated methods are also very diverse such as sol-gel, hydrothermal, wet chemistry, hydrothermal ultrasound, co-precipitation,...²³⁻³¹. The material's properties and application areas depend on material morphology and fabricated method. In order to enhance the application range of ZnO materials that respond to both ultraviolet and visible light regions, ZnO nanostructured materials are modified by single doping or co-doping with transition metal ions, noble metal ions, or rare earth metal ions, or composite or hybrid materials to change the shape and reduce the particle size of the materials^{7-9,18-31}.

In this study, we fabricate ZnO nanostructured materials co-doped with Co^{2+} and Ni^{2+} ions and undoped ZnO materials by low-temperature hydrothermal method and investigate the photocatalytic prop-

Cite this article : Dung T N, Mai N T T, Chinh H D. **Study on the fabrication and investigation of the structural, optical and photocatalytic properties of Co^{2+} , Ni^{2+} co-doped ZnO nanomaterials.** *Sci. Tech. Dev. J. – Engineering and Technology* 2024; 6(S13):73-79.

erties for methylene blue (MB) dye solution decomposition under visible light radiation.

MATERIALS AND METHODS

Chemicals

Zinc acetate dihydrate ($\text{Zn}(\text{CH}_3\text{COO})_2 \cdot 2\text{H}_2\text{O}$ 99%, AR-China); Cobalt(II) sulfate heptahydrate ($\text{CoSO}_4 \cdot 7\text{H}_2\text{O}$ 99.5%, AR-China) Nickel(II) nitrate hexahydrate ($\text{Ni}(\text{NO}_3)_2 \cdot 6\text{H}_2\text{O}$ 98%, AR-China) Sodium hydroxide (NaOH 98%, AR-China); Ethanol (alcohol, $\text{C}_2\text{H}_5\text{OH}$ 99.7%, AR-China), double distilled water.

Experimental process

A mixed solution of 60 ml include 0.1M solution of $\text{Zn}(\text{CH}_3\text{COO})_2$ and 0.1M solution of sodium hydroxide was mixed in a volume ratio of 1:1 and was stirred evenly on a magnetic stirrer for 20 min. Next, the calculated salt amount of $\text{CoSO}_4 \cdot 7\text{H}_2\text{O}$ and $\text{Ni}(\text{NO}_3)_2 \cdot 6\text{H}_2\text{O}$ was added to the above mixed solution with a molar percentage of Co^{2+} ion (1 mol%) and Ni^{2+} ion (2 mol%) (compared to the number of moles of Zn^{2+} in the solution). Continue to stir the above mixed solution evenly for another 20 min. Then, hydrothermally heated at 90°C for 12h. The paste mixture after hydrothermal process was filtered and washed thoroughly with distilled water and absolute alcohol. This clean paste was next dried at 90°C for 24h. The product obtained was a fine ZnO paste powder co-doped with 1 mol% Co^{2+} and 2 mol% Ni^{2+} and was denoted ZnO-1%Co-2%Ni. An undoped ZnO material sample was prepared with the same above process but without the addition of $\text{CoSO}_4 \cdot 7\text{H}_2\text{O}$ and $\text{Ni}(\text{NO}_3)_2 \cdot 6\text{H}_2\text{O}$ salts, resulting in an undoped ZnO sample, which was denoted ZnO, used in experiments for comparison. Figure 1 was the ZnO-1%Co-2%Ni and ZnO paste powder sample after hydrothermal process at 90°C for 12h.

The characterization of Co^{2+} , Ni^{2+} co-doped ZnO materials (ZnO-1%Co-2%Ni) was measured by the following methods: X-ray diffraction method (XRD, X'pert Pro), Cu-K α radiation ($\lambda = 1.54065 \text{ \AA}$), scanning angle $2\theta \gg 25\text{-}75^\circ$; Scanning electron microscopy, X-ray energy scattering spectroscopy (SEM/ EDX, HITACHI TM4000 Plus); solid UV-Vis absorption/reflectance spectra (Jasco V-750), scanning speed 200 nm/min.

Photocatalytic experiments: Accurately weigh 0.015g of each sample of photocatalysts ZnO-1%Co-2%Ni and ZnO. Next, put each powder sample into a pyrex glass beaker containing 60 mL of MB solution with a concentration of 10 ppm. This reaction dye solution was stirred and left completely dark for 1 hour

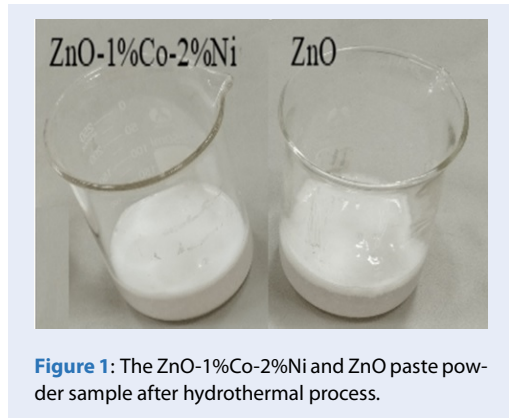


Figure 1: The ZnO-1%Co-2%Ni and ZnO paste powder sample after hydrothermal process.

to achieve adsorption and desorption equilibrium. Next, the solution was irradiated under a visible light source (using Osram 220V-250W lamp, Philip brand) at room temperature. At each survey period, took out 2 mL of the solution and measure the absorbance on a UV-Vis photometer system (Agilent 8453) at a max wavelength (664 nm). The remaining content (%) of MB dye after the photocatalytic decomposition process was determined according to the following formula (in which, C_o and C_t were the initial and after a certain irradiation time (t) MB dye solution concentration, respectively).

$$\text{The remaining content (\%)} = (C_t/C_o) \times 100 \quad (1)$$

RESULTS AND DISCUSSION

Structural characterization of materials

The results of the X-ray diffraction spectra of the ZnO-1%Co-2%Ni and ZnO samples were shown in Figure 2. The XRD spectra presented that the ZnO-1%Co-2%Ni and ZnO samples both appear peaks at the diffraction angle site $2\theta \gg 31.7^\circ, 34.3^\circ, 36.2^\circ, 47.45^\circ, 56.6^\circ, 62.8^\circ$ and 67.25° which attributed to the lattice planes of (100), (002), (101), (102), (110), (103) and (112) of ZnO hexagonal wurtzite structure with space group $P63mc$ ^{8,20}. On the other hand, on the XRD spectra, no other strange peaks were observed, which were attributed to Co or Ni elements or compounds of those elements^{19,20,22,31}. So, it could be seen that the ZnO-1%Co-2%Ni and ZnO material samples were hexagonal wurtzite ZnO single-phase, and the Co^{2+} and Ni^{2+} ions had been successfully doped into the ZnO material in the form of replacing the Zn^{2+} ion site. This could also be easily seen because the doped elements (Co and Ni) all had ionic radii that were approximately the same as the radius of Zn^{2+} ion ($r(\text{Zn}^{2+}) = 0.74 \text{ \AA}$, $r(\text{Co}^{2+}) = 0.72 \text{ \AA}$, $r(\text{Ni}^{2+}) = 0.70 \text{ \AA}$)^{19,20,22,31}.

The average crystallite size of the ZnO-1%Co-2%Ni and ZnO samples was calculated by applying the Scherrer equation^{6,7}:

$$D = K\lambda / \lambda \cos \theta \tag{1}$$

In which, D is the average crystal size; K is a coefficient that depends on the shape of the crystal $K = 0.9$; $\lambda = 1.54056 \text{ \AA}$ is the diffraction wavelength; β is the full width at half maximum (FWHM), θ is the diffraction angle at the position of the (101) diffraction plane. The calculation results showed that the average crystal sizes of the ZnO-1%Co-2%Ni and ZnO samples were 25.06 nm and 29.48 nm, respectively. Thus, the 1%Co²⁺, 2%Ni²⁺ co-doped ZnO sample had reduced the average crystal size more than the undoped ZnO sample. This further confirms that the Co²⁺ and Ni²⁺ ions had interacted and were doped into the crystal lattice of ZnO.

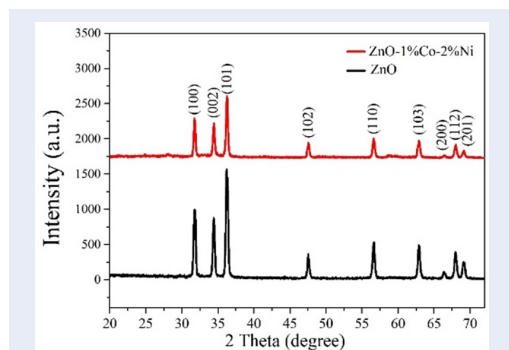


Figure 2: The X-ray diffraction spectra (XRD) of ZnO-1%Co-2%Ni and ZnO samples

Material surface morphology

Figure 3 was a scanning electron microscope (SEM) of ZnO-1%Co-2%Ni and ZnO samples. The SEM image indicated that the surface of the ZnO sample had a thin flake shape. The ZnO-1%Co-2%Ni sample had the form of small particles that were gradually separated from the thin flakes and was distributed relatively uniform on the surface. Thus, the surface state of ZnO-1%Co-2%Ni sample was changed the compared to undoped ZnO sample. This showed the possibility of changing the photocatalytic properties of doped ZnO materials compared to undoped ZnO.

Figure 4 was the X-ray energy scattering spectra of ZnO-1%Co-2%Ni and ZnO samples.

The EDX spectra of ZnO sample indicated that only the spectral peaks of the two Zn and O elements that made up the ZnO material were observed. In the

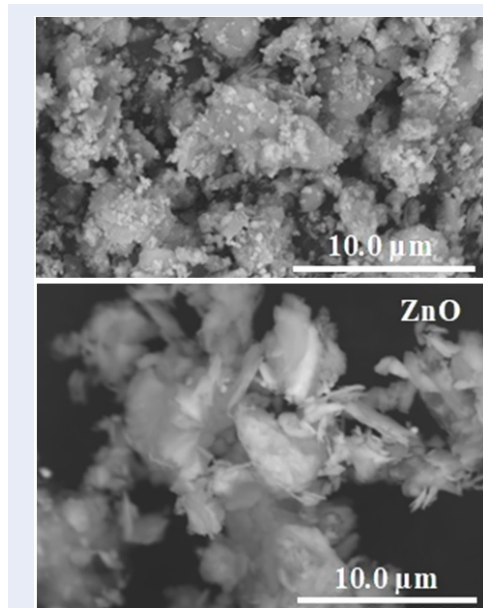


Figure 3: The scanning electron microscope (SEM) of the ZnO-1%Co-2%Ni and ZnO samples

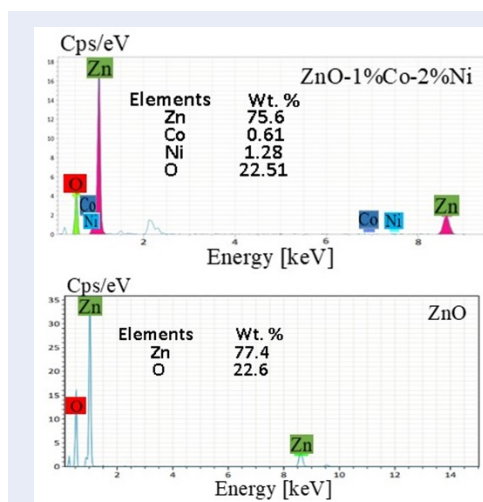


Figure 4: The X-ray energy scattering spectra (EDX) of the ZnO-1%Co-2%Ni and ZnO samples

ZnO-1%Co-2%Ni sample, it showed that in addition to the Zn and O elements, there were also spectral peaks with low intensity of the two Co and Ni elements. Thus, it could be seen that the ZnO sample was fabricated in the form of pure wurtzite ZnO phase. The ZnO-1%Co-2%Ni sample was also in the form of pure wurtzite ZnO phase but was doped into the ZnO crystal lattice by two Co and Ni elements.

UV-vis absorption spectra and function plot $d(F(R)h)/dE$ with energy h (Kubelka–Munk)

Figure 5 was the Uv-vis spectra of ZnO-1%Co-2%Ni and ZnO samples. On the Uv-vis spectra indicated that ZnO sample had an absorption edge in the ultraviolet region ($\lambda \leq 385\text{nm}$). The ZnO-1%Co-2%Ni sample had an absorption edge that was broadened and shifted toward visible light region ($\lambda \gg 400\text{nm}$). It could be seen that ZnO sample would only be capable to achieve applications photoexcited of light in the ultraviolet region. The ZnO-1%Co-2%Ni sample would provide the possibility to achieve applications photoexcited of light in the visible region¹⁸.

Applying the Kubelka-Munk (K-M) method to further exploit the optical properties of the material, the E_g value of samples were determined by extrapolation according to the K-M equation¹⁸ as follows.

$$d[\ln(F(R) \times hv)]/d(hv) = n/(hv - E_g) \quad (3)$$

In which, $F(R)$ was a function of the diffuse reflectance coefficient determined from the diffuse reflectivity coefficient R to $F(R) = (1-R)^2/2R$; $h\nu$ was the photon energy variable; E_g was the optical gap energy. The E_g value of samples were extrapolated from the function plot of $d[\ln(F(R)hv)](hv)$ vs $h\nu$ energy (Figure 6). The extrapolation results for the optical gap energy values of the ZnO-1%Co-2%Ni and ZnO samples were 3.17 eV and 3.34 eV, respectively. The E_g value of the ZnO-1%Co-2%Ni sample was shown to be smaller than that of the ZnO sample and also smaller than that of bulk ZnO (3.37 eV)^{1,2}. These E_g values of the samples were found to be consistent with their solid Uv-vis spectra (Figure 5) This demonstrated the possibility of achieving light-excited optical applications in the visible region of the ZnO sample doped by 1%Co²⁺ and 2%Ni²⁺ ions.

Investigation of photocatalytic properties

Figure 7a was the plot surveying the MB dye remaining content (%) after photocatalytic decomposition process under visible light exposure time of ZnO-1%Co-2%Ni and ZnO samples.

The plot (Figure 7a) showed that ZnO-1%Co-2%Ni sample had a MB remaining content of 12.38% (corresponding to achieving a photocatalytic efficiency for MB decomposition of 87.62% after 3.5 h of visible light exposure). The ZnO sample almost could not MB decompose, the MB remaining content was 81.85% (corresponding to only achieving a photocatalytic efficiency for MB decomposition of 18.48%). Therefore, it could be said that ZnO-1%Co-2%Ni

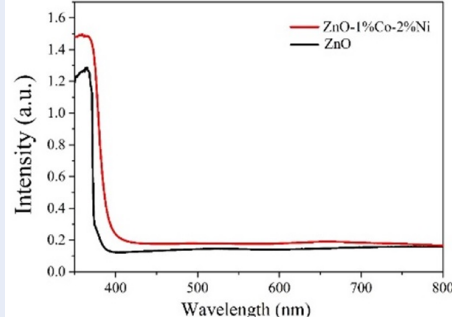


Figure 5: The solid Uv-vis absorption spectra of the ZnO-1%Co-2%Ni and ZnO samples

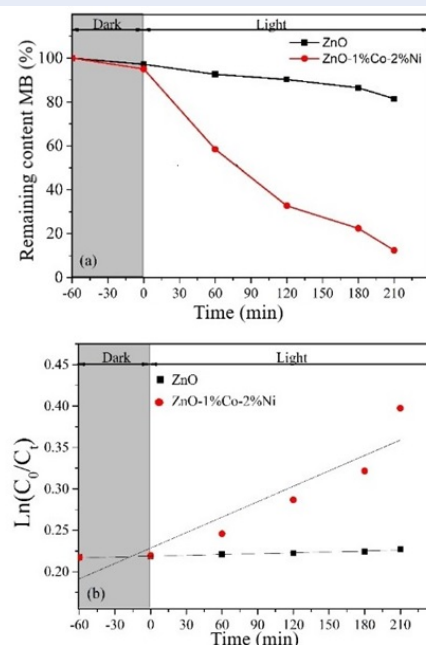


Figure 7: a- The MB dye remaining content at irradiation time; b- Kinetic decomposition of MB dye solution through the linear relationship of the plot $\ln(C_0/C_t)$ vs visible light irradiation time of ZnO-1%Co-2%Ni and ZnO samples

sample has achieved superior properties compared to the undoped ZnO sample, that is, it has allowed to achieve effective photocatalytic decomposition of MB dye solution in the visible light.

The rate constant for the photocatalytic decomposition reaction of MB dye was determined based on the Langmuir-Hinshelwood (L-H) kinetic model^{7,21} as follows

$$\ln(C_0/C_t) = kt \quad (4)$$

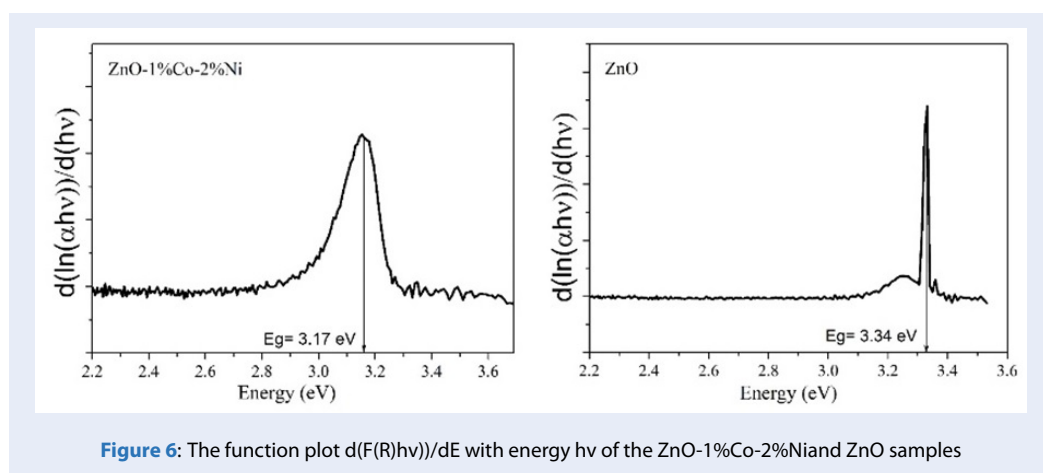


Figure 6: The function plot $d(F(R)hv)/dE$ with energy hv of the ZnO-1%Co-2%Ni and ZnO samples

Where C_o and C_t are the initial and concentration of MB at a certain time interval and k is the rate constant. On the L-H kinetic model (Figure 7b) showed that the plot of $\ln(C_o/C_t)$ vs time followed a linear relationship (first order function) with a quite good R^2 correlation coefficient ($R^2 \geq 0.92$). The k rate constant of ZnO-1%Co-2%Ni and ZnO samples was determined as 0.0006204 and 0.00003471 min^{-1} , respectively. It was found that the k rate constant of ZnO-1%Co-2%Ni sample was many times larger than that of undoped ZnO sample. The rate constant k shows that the larger its value, the faster the rate efficiency for the MB dye decomposition reaction.

CONCLUSION

Experiments had successfully fabricated ZnO-1%Co-2%Ni and ZnO nanostructured materials at low temperatures. The fabricated samples had a hexagonal wurtzite structure. The ZnO-1%Co-2%Ni sample had reduced the average crystal size more than the undoped ZnO sample. The average crystal sizes of the ZnO-1%Co-2%Ni and ZnO samples were 25.06 and 29.48 nm, respectively. The optical gap energy (calculated according to the K-M method) of ZnO-1%Co-2%Ni sample (3.17 eV) was smaller than that of ZnO sample (3.34 eV). The ZnO-1%Co-2%Ni sample achieved the ability for decompose MB dye solution under visible light. The undoped ZnO sample had almost no effect on decomposing MB under visible light. The MB decomposition rate constant of ZnO-1%Co-2%Ni and ZnO samples followed a first-order kinetic model with good correlation coefficient ($R^2 \geq 0.92$). The rate constant of ZnO-1%Co-2%Ni sample (0.006204 min^{-1}) was much larger than that of undoped ZnO sample (0.0003471 min^{-1}).

ACKNOWLEDGMENT

This work was funded by Hanoi University of Science and Technology (HUST) under the project number CT2022.04.BKA.05, Science and Technology Project of the Ministry of Education and Training of Vietnam.

CONFLICT OF INTEREST

The authors would like to confirm that there is no conflict of interest in publishing the article.

CREDIT AUTHORSHIP CONTRIBUTION STATEMENT

Ta Ngoc Dung: Methodology, Formal analysis, Supervision; Nguyen Thi Tuyet Mai: Investigation, original draft, Formal analysis, Supervision; Huynh Dang Chinh: Methodology, Formal analysis, Supervision.

REFERENCES

- Xu S, Wang ZL. One-Dimensional ZnO Nanostructures: Solution Growth and Functional Properties. *Nano Res.* 2011;4(11):1013-1098; Available from: <https://doi.org/10.1007/s12274-011-0160-7>.
- Look D. Recent Advances in ZnO Materials and Devices. *Mater Sci Eng B.* 2001;80(1-3):383-387; Available from: [https://doi.org/10.1016/S0921-5107\(00\)00604-8](https://doi.org/10.1016/S0921-5107(00)00604-8).
- Iwasaki M, Inubushi Y, Ito S. New route to prepare ultrafine ZnO particles and its reaction mechanism. *J Mater Sci Lett.* 1997;16:1503-1505; Available from: <https://doi.org/10.1023/A:1018566923329>.
- Richa B, Amardeep B, Jitendra PS, Keun HC, Navdeep G. Structural and electronic investigation of ZnO nanostructures synthesized under different environments. *Heliyon.* 2018;4:e00594; PMID: 29862357. Available from: <https://doi.org/10.1016/j.heliyon.2018.e00594>.
- Lee KM, Lai CW, Ngai KS, Juan JC. Recent developments of zinc oxide based photocatalyst in water treatment technology: A review. *Water Res.* 2016;88:428-448; PMID: 26519627. Available from: <https://doi.org/10.1016/j.watres.2015.09.045>.
- Kulkarni AV, Chavhan A, Bappakhane A, Chimmankar J. ZnO Nanoparticles as Adsorbent for Removal of Methylene Blue dye. *Res J Chem Environ Sci.* 2016;4(4S):158-163;.

7. Rahmah MI, Sabry RS, Aziz WJ. Synthesis and study photocatalytic activity of Fe₂O₃-doped ZnO nanostructure under visible light irradiation. *Int J Environ Anal Chem.* 2020;1-14; Available from: <https://doi.org/10.1080/10667857.2019.1681717>.
8. Ngullie RC, Alaswad SO, Bhuvaneshwari K, Shanmugam P, Pazhanivel T, Arunachalam P. Synthesis and Characterization of Efficient ZnO/g-C₃N₄ Nanocomposites Photocatalyst for Photocatalytic Degradation of Methylene Blue. *Coatings.* 2020;10:500; Available from: <https://doi.org/10.3390/coatings10050500>.
9. Dhara A, Sain S, Das S, Pradhan SK. Microstructure, optical, dielectric and electrical characterizations of Mn doped ZnO nanocrystals synthesized by mechanical alloying. *Ceram Int.* 2018;44(6):110-112; Available from: <https://doi.org/10.1016/j.ceramint.2018.01.151>.
10. Wang ZL. Zinc oxide nanostructures: growth, properties and applications. *J Phys Condens Matter.* 2004;16:R829; Available from: <https://doi.org/10.1088/0953-8984/16/25/R01>.
11. Mende LS, et al. ZnO - nanostructures, defects, and devices. *Mater Today.* 2007;10(5):40-48; Available from: [https://doi.org/10.1016/S1369-7021\(07\)70078-0](https://doi.org/10.1016/S1369-7021(07)70078-0).
12. Gu P, Wang X, Li T, Meng H. Synthesis, characterization and photoluminescence of ZnO spindles by polyvinylpyrrolidone-assisted low-temperature wet-chemistry process. *J Cryst Growth.* 2012;338(1):162-165; Available from: <https://doi.org/10.1016/j.jcrysgro.2011.10.028>.
13. Suwanboon S. Structural and Optical Properties of Nanocrystalline ZnO Powder from Sol-Gel Method. *ScienceAsia.* 2008;34(1):31-34; Available from: <https://doi.org/10.2306/scienceasia1513-1874.2008.34.031>.
14. Geetha D, Thilagavathi T. Hydrothermal Synthesis Of Nano ZnO Structures From CTAB. *J Nanomater Biostruct.* 2010;5(1):297-301;
15. Thilagavathi T, Geetha D. Nano ZnO structures synthesized in presence of anionic and cationic surfactant under hydrothermal process. *Appl Nanosci.* 2012;4(2):127-132; Available from: <https://doi.org/10.1007/s13204-012-0183-8>.
16. Li P, Liu H, Fang-xiang X, Wei Y. Controllable growth of ZnO nanowhiskers by a simple solution route. *Mater Chem Phys.* 2008;112(2):393-397; Available from: <https://doi.org/10.1016/j.matchemphys.2008.05.065>.
17. Yacine C, Ahcène C, Yannick L, Mohammed R, Abdelaziz K, Christian C. Electrical, dielectric and photocatalytic properties of Fe-doped ZnO nanomaterials synthesized by sol gel method. *Process Appl Ceram.* 2016;10(3):125-135; Available from: <https://doi.org/10.2298/PAC1603125C>.
18. Wibowo JA, et al. Cu- and Ni-Doping Effect on Structure and Magnetic Properties of Fe-Doped ZnO Nanoparticles. *Adv Mater Phys Chem.* 2013;3:48-57; Available from: <https://doi.org/10.4236/ampc.2013.31008>.
19. Nair MG, Nirmala M, Rekha K, Anukalini A. Structural, Optical, Photo Catalytic and Antibacterial Activity of ZnO and Co Doped ZnO Nanoparticles. *Mater Lett.* 2011;65(12):1797-1800; Available from: <https://doi.org/10.1016/j.matlet.2011.03.079>.
20. Yildirim OA, Arslan H, Sönmezoğlu S. Facile synthesis of cobalt-doped zinc oxide thin films for highly efficient visible light photocatalysts. *Appl Surf Sci.* 2016;390:111-121; Available from: <https://doi.org/10.1016/j.apsusc.2016.08.069>.
21. Gnanaprakasam A, Sivakumar VM, Thirumarimurugan M. A study on Cu and Ag doped ZnO nanoparticles for the photocatalytic degradation of brilliant green dye: synthesis and characterization. 2016;74(6):1426-1435; PMID: 27685972. Available from: <https://doi.org/10.2166/wst.2016.275>.
22. Pal B, Giri PK. Defect mediated magnetic interaction and high T_c ferromagnetism in Co doped ZnO nanoparticles. *J Nanosci Nanotechnol.* 2011;11(10):1-8; PMID: 22400318. Available from: <https://doi.org/10.1166/jnn.2011.4293>.
23. Wang WW, Zhu YJ. Shape-controlled synthesis of zinc oxide by microwave heating using an imidazolium salt. *Inorg Chem Commun.* 2004;7:1003-1005; Available from: <https://doi.org/10.1016/j.inoche.2004.06.014>.
24. Thilagavathi T, Geetha D. Nano ZnO structures synthesized in presence of anionic and cationic surfactant under hydrothermal process. *Appl Nanosci.* 2012;7 pages; Available from: <https://doi.org/10.1007/s13204-012-0183-8>.
25. Yahiyaa LZ, Dhahir MK, Mahdi ZF. Synthesized ZnO Nanorod with Different Range of Morphologies Using a Simple Hydrothermal Method. *AIP Conf Proc.* 2020;2290:030022; Available from: <https://doi.org/10.1063/5.0031634>.
26. Jeyachitra, Senthilnathan V, Senthil TS. Studies on electrical behavior of Fe doped ZnO nanoparticles prepared via co-precipitation approach for photo-catalytic application. *J Mater Sci Mater Electron.* 2017; Available from: <https://doi.org/10.1007/s10854-017-8021-0>.
27. Wang Y, Ma Q, Jia H, Wang Z. One-step solution synthesis and formation mechanism of flower-like ZnO and its structural and optical characterization. *Ceram Int.* 2016;42:10751-10757; Available from: <https://doi.org/10.1016/j.ceramint.2016.03.200>.
28. Sathya B, Porkalai V, Anburaj DB, Nedunchezian G. Low Temperature Ferromagnetism and Optical Properties of Fe Doped ZnO Nanoparticles Synthesized by Sol-Gel Method. *Mech Mater Sci Eng.* 2017;6 pages; Available from: <https://doi.org/10.4028/www.scientific.net/NHC.17.101>.
29. Panigrahy B, et al. Aqueous Synthesis of Mn- and Co-Doped ZnO Nanorods. *J Phys Chem C.* 2010;114:11758-11763; Available from: <https://doi.org/10.1021/jp102163b>.
30. Cherif Y, et al. Electrical, dielectric and photocatalytic properties of Fe-doped ZnO nanomaterials synthesized by sol gel method. *Process Appl Ceram.* 2016;10(3):125-135; Available from: <https://doi.org/10.2298/PAC1603125C>.
31. Ali M, et al. Preparation of Co and Ni Doped ZnO Nanoparticles served as Encouraging Nano-Catalytic Application. *Mater Res.* 2019;6:1-18; Available from: <https://doi.org/10.1088/2053-1591/ab6383>.

Nghiên cứu chế tạo và khảo sát các đặc tính cấu trúc, tính chất quang và xúc tác quang của vật liệu cấu trúc nano ZnO pha tạp đồng thời Co^{2+} , Ni^{2+}

Tạ Ngọc Dũng, Nguyễn Thị Tuyết Mai*, Huỳnh Đăng Chính

TÓM TẮT

Trong nghiên cứu này đã chế tạo thành công vật liệu cấu trúc nano ZnO pha tạp đồng thời Co^{2+} , Ni^{2+} (Co,Ni-ZnO NMs) bằng phương pháp thủy nhiệt ở nhiệt độ thấp ở 90°C trong 12 giờ. Các ion Co^{2+} và Ni^{2+} được pha tạp vào vật liệu nano ZnO với tỷ lệ theo số mol lần lượt là 1 % và 2 % (được tính toán so với số mol của ion Zn^{2+}). Các phương pháp nghiên cứu để xác định các đặc tính cấu trúc, tính chất quang và tính chất xúc tác quang phân hủy chất màu methylene blue (MB) được sử dụng như là XRD, SEM, EDX, UV-vis rắn/lỏng. Kết quả khảo sát cho thấy, vật liệu chế tạo ở dạng cấu trúc đơn pha wurtzite với kích thước hạt tinh thể nano-mét. Năng lượng khe trống quang được xác định theo phương trình Kubelka–Munk và đạt được cỡ 3,17 eV nhỏ hơn so với ZnO không pha tạp (3,34 eV). Điều này là mong muốn trong nghiên cứu về vật liệu bán dẫn để cải thiện tính ứng dụng của vật liệu kích thích được ánh sáng dịch chuyển về vùng nhìn thấy. Đồng thời kết quả khảo sát cũng cho thấy vật liệu nano ZnO pha tạp đồng thời Co^{2+} , Ni^{2+} đạt được hiệu quả xúc tác quang phân hủy chất màu methylene blue (MB) trong vùng ánh sáng nhìn thấy. Như vậy, vật liệu ZnO pha tạp đồng thời các ion Co^{2+} và Ni^{2+} đã đạt được tính ưu việt trong những ứng dụng quang học được kích thích bởi ánh sáng khả kiến (vật liệu ZnO không pha tạp chỉ đạt được ứng dụng quang học trong vùng ánh sáng tử ngoại). Hằng số tốc độ của phản ứng phân hủy quang xúc tác đối với thuốc nhuộm MB đã được xác định theo mô hình động học Langmuir Hinshelwood (L-H). Hằng số tốc độ phân hủy này của các mẫu chế tạo đều tuân theo mô hình động học bậc nhất với hệ số tương quan R^2 cao (đạt trên 0,92). Hằng số tốc độ của mẫu Co,Ni-ZnO NMs lớn hơn khoảng 17,8 lần so với mẫu ZnO không pha tạp (đạt lần lượt là 0,006204 và 0,0003471 phút^{-1}).

Từ khóa: Cấu trúc nano Wurtzite ZnO, ZnO pha tạp đồng thời Co^{2+} , Ni^{2+} , Kubelka–Munk, ánh sáng nhìn thấy

Trường Hóa và Khoa học sự sống, Đại học Bách Khoa Hà Nội, số 1 Đại Cồ Việt Hà Nội, Việt Nam

Liên hệ

Nguyễn Thị Tuyết Mai, Trường Hóa và Khoa học sự sống, Đại học Bách Khoa Hà Nội, số 1 Đại Cồ Việt Hà Nội, Việt Nam

Email: mai.nguyenthituyet@hust.edu.vn

Lịch sử

- Ngày nhận: 01-10-2023
- Ngày chấp nhận: 10-1-2024
- Ngày đăng: 31-3-2024

DOI : <https://doi.org/10.32508/stdjet.v6iS13.1256>



Bản quyền

© ĐHQG Tp.HCM. Đây là bài báo công bố mở được phát hành theo các điều khoản của the Creative Commons Attribution 4.0 International license.



Trích dẫn bài báo này: Dũng T N, Mai N T T, Chính H D. Nghiên cứu chế tạo và khảo sát các đặc tính cấu trúc, tính chất quang và xúc tác quang của vật liệu cấu trúc nano ZnO pha tạp đồng thời Co^{2+} , Ni^{2+} . *Sci. Tech. Dev. J. - Eng. Tech.* 2024, 6(S13):73-79.